Three-Dimensional Analysis of Vestibular Efferent Neurons Innervating Semicircular Canals of the Gerbil

I. M. PURCELL[1] AND A. A. PERACHIO[1,2,3]
[1]*Department of Otolaryngology,* [2]*Physiology and Biophysics,* [3]*Anatomy and Neurosciences, University of Texas Medical Branch, Galveston, Texas 77555-1063*

Purcell, I. M. and A. A. Perachio. Three-dimensional analysis of vestibular efferent neurons innervating semicircular canals of the gerbil. *J. Neurophysiol.* 78: 3234–3248, 1997. Anterograde labeling techniques were used to examine peripheral innervation patterns of vestibular efferent neurons in the crista ampullares of the gerbil. Vestibular efferent neurons were labeled by extracellular injections of biocytin or biotinylated dextran amine into the contralateral or ipsilateral dorsal subgroup of efferent cell bodies (group e) located dorsolateral to the facial nerve genu. Anterogradely labeled efferent terminal field varicosities consist mainly of boutons en passant with fewer of the terminal type. The bouton swellings are located predominately in apposition to the basolateral borders of the afferent calyces and type II hair cells, but several boutons were identified close to the hair cell apical border on both types. Three-dimensional reconstruction and morphological analysis of the terminal fields from these cells located in the sensory neuroepithelium of the anterior, horizontal, and posterior cristae were performed. We show that efferent neurons densely innervate each end organ in widespread terminal fields. Subepithelial bifurcations of parent axons were minimal, with extensive collateralization occurring after the axons penetrated the basement membrane of the neuroepithelium. Axonal branching ranged between the 6th and 27th orders and terminal field collecting area far exceeds that of the peripheral terminals of primary afferent neurons. The terminal fields of the efferent neurons display three morphologically heterogeneous types: central, peripheral, and planum. All cell types possess terminal fields displaying a high degree of anisotropy with orientations typically parallel to or within ±45° of the longitudinal axis if the crista. Terminal fields of the central and planum zones predominately project medially toward the transverse axis from the more laterally located penetration of the basement membrane by the parent axon. Peripheral zone terminal fields extend predominately toward the planum semilunatum. The innervation areas of efferent terminal fields display a trend from smallest to largest for the central, peripheral, and planum types, respectively. Neurons that innervate the central zone of the crista do not extend into the peripheral or planum regions. Conversely, those neurons with terminal fields in the peripheral or planum regions do not innervate the central zone of the sensory neuroepithelium. The central zone of the crista is innervated preferentially by efferent neurons with cell bodies located in the ipsilateral group e. The peripheral and planum zones of the crista are innervated preferentially by efferent neurons with cell bodies located in the contralateral group e. A model incorporating our anatomic observations is presented describing an ipsilateral closed-loop feedback between ipsilateral efferent neurons and the periphery and an open-loop feedforward innervation from contralateral efferent neurons. A possible role for the vestibular efferent neurons in the modulation of semicircular canal afferent response dynamics is proposed.

INTRODUCTION

The vestibular sensory neuroepithelia contains terminals of neurons the cell bodies of which are located bilaterally in the brain stem. Those vestibular efferent neurons ostensibly provide modulatory control over the hair cell and afferent neuron's transduction process. It has been proposed that these neurons affect the resting discharge and sensitivity of certain subpopulations of vestibular afferent neurons to angular and linear head accelerations (Boyle and Highstein 1990; Boyle et al. 1991; Brichta and Goldberg 1996; Goldberg and Fernandez 1980; Highstein 1991; McCue and Guinan 1994; Rossi and Martini 1991).

The mammalian vestibular end organs receive direct bilateral innervation from two groups of efferent neurons in the medullary brain stem. In the gerbil, the larger of the two (<200 cell bodies), is a collection of choline acetyltransferase (ChAT), acetylcholinesterase, calcitonin gene-related peptide (CGRP), and enkephalin mRNA positive cells, located dorsolateral to the genu of the seventh nerve, ventral and medial to the vestibular nuclei (Perachio and Kevetter 1989; Ryan et al. 1991). The smaller group, staining negative for the above markers, is located immediately ventral to the genu. The entire vestibular efferent nuclear group has been called the *group e* (Goldberg and Fernandez 1980). In gerbil, the largest number of labeled efferent neurons observed after unilateral horseradish peroxidase labyrinth injection was 218 somatae. Of these, 56% were located contralateral to the injected labyrinth and 11% were located in the smaller ventral group (Perachio and Kevetter 1989). Double retrograde labeling studies in mammals (Dechesne et al. 1984) report as many as 20% of vestibular efferent cells project to both labyrinths. The bilateral symmetric origin and predominant contralateral location of the gerbil vestibular efferent neurons is consistent with reports in other mammals (Dechesne et al. 1984; Gacek and Lyon 1974; Goldberg and Fernandez 1980; Marco et al. 1993; Schwarz et al. 1987; Warr 1975). On entering the labyrinth, some of the axons collateralize to various end organs (Gacek 1982; Schwarz et al. 1981). Autoradiographic (Raymond and Dememes 1983), immunohistochemical (Tanaka et al. 1988; Usami et al. 1987), and direct ultrastructural examinations of efferent bouton terminals in the sensory neuroepithelium (Goldberg et al. 1990; Sans and Highstein 1984; Smith and Rasmussen 1968) suggest that a few efferent parent axons give rise to extensive collateralized innervation.

Regional differences in efferent innervation have been identified previously in the mammalian crista ampullares. Radioautographic labeling (Raymond and Dememes 1983) of the vestibular sensory neuroepithelium in cat revealed a symmetrical ''periphery-apex'' arrangement, with higher labeling density occurring in the peripheral regions (compared with apex) after ''efferent neuron cluster'' injections

contralateral to the labyrinth. The highest apex labeling density was observed after ipsilateral injections. Usami et al. (1987) examined squirrel monkey cristae ampullares for γ-aminobutyric acid (GABA) labeling. Although not quantified, immunopositive efferent bouton-like endings and fibers were observed predominately in the peripheral regions. Although immunolabeling studies in the rat crista (Tanaka et al. 1988) reported a uniform distribution of fibers containing the efferent neuropeptide CGRP, only calyx-type synaptic profiles were identified as receiving innervation (Ohno et al. 1993; Tanaka et al. 1989). In contrast, studies in rat and human (Ishiyama et al. 1994; Wackym 1993) revealed uniform labeling of CGRP and ChAT localized around both afferent calyces and type II hair cells.

The physiological influences of the efferent neurons is suggested by findings primarily related to the responses of afferent neurons to artificial stimulation of the mammalian efferent pathway. Goldberg and Fernandez (1980) demonstrated, for squirrel monkey afferents, that galvanic stimulation of the efferent pathway primarily produces an excitatory effect on afferent background discharge. Further, they found that the most responsive cells were those characterized by irregular discharge and comparatively high gain (impulses/second of neuron firing per degree/second of table rotation) responses to head acceleration. In more recent work, evidence from studies in squirrel monkey (Lysakowski et al. 1995) and chinchilla (Baird et al. 1988; Fernandez et al. 1988) indicates that irregularly firing higher gain dimorphic and low gain calyx-only afferents innervate the central zones of the cristae, and that lower gain more regularly firing dimorphic and low gain regularly firing bouton-only afferent neurons innervate the noncentral regions of the semicircular canal cristae.

The combined morphological and physiological findings give rise to several questions: are there different morphological types of efferent endings in terms of their site of termination and the distribution of their terminal fields? Are there any morphological distinctions between the innervation pattern of neurons arising from ipsilateral or contralateral efferent nuclei? Is there a relationship between the site of termination of efferent innervation of the cristae and the regional distribution of the two types of hair cells and of the known classes of afferent terminals?

These questions were addressed by analyzing the morphological features and regional distributions of individual efferent neurons innervating the sensory neuroepithelium of the semicircular canals. The results of our morphological examination were used to develop a simple model that predicts how the bilateral efferent innervation of the canals may influence afferent activity during active head movements. Some of our data have appeared previously in abstract form (Purcell and Perachio 1996).

METHODS

Species

Forty-eight gerbils (*Meriones unguiculatus*) of both sexes and weighing from 60 to 70 g were used in the present study. All surgery was performed under aseptic conditions with general anesthesia. Gerbils were anesthetized with an intraperitoneal injection of pentobarbital sodium (Nembutal 25 mg/kg) followed within 5 min by an intramuscular injection of ketamine (25 mg/kg). Supplementary doses of ketamine were administered as needed to maintain anesthesia. Core body temperature as measured by a thermistor rectal probe was maintained in a range of 36.5–38°C by a sodium acetate heating pad. Before placement into a stereotaxic frame, the animals' eyes were coated with ophthalmic ointment and the scalp was shaved. The head was mounted in the standard position in the stereotaxic frame with the incisor bar secured 8 mm below the zero ear bar plane of the instrument. This positioned the nose tilted down 20° with respect to the interaural axis to align the major plane of the horizontal semicircular canals coplanar with the earth horizontal plane. A midsagittal incision was made exposing the dorsal calvaria.

Injection of biocytin and biotinylated dextran amine

CONTRALATERAL BRAIN STEM INJECTIONS. In 28 gerbils, unilateral extracellular injections were made near the dorsal group e with solutions of the tracer biocytin. A 0.6-mm dental burr was used to expose the dorsal aspect of the cerebellum. The dura mater then was removed over the cerebellar cortex and the surface kept moist with artificial cerebral spinal fluid. A glass microcapillary pipette filled with a solution of 5% biocytin (Sigma) in 0.05 M Tris (pH 8.3) and a tip broken to a final diameter of 20 μm was placed stereotaxically 50–100 μm above the dorsal cluster of the gerbil efferent neurons (Fig. 1) (Perachio and Kevetter 1989). Biocytin was ejected from the tip ionophoretically by passing direct anodal (+) current, 3–5 μA, for 10 min. After completion of the extracellular injection, the electrode was withdrawn and the wound closed. After a survival time of 18–24 h, a length of time sufficient enough to allow transport of the label, the animals were anesthetized deeply with urethan (0.7 ml, 500 mg/kg ip) and perfused transcardially with warmed gerbil Ringer saline followed by a cold solution of fixative containing 4% paraformaldehyde and 0.5% glutaraldehyde in 0.1 M phosphate buffer (pH 7.6). Within 3.5 min of the start of the perfusion, the ampullae of the contralateral horizontal, superior, and posterior canals were exposed and directly bathed in fixative for 1 h. The individual cristae then were dissected out carefully using a fine microhook and placed in phosphate buffer (0.1 M, pH 7.4). The pigmented epithelium and membranous labyrinth of the crista ampullares were teased carefully from the sensory neuroepithelium to allow maximal visualization of the labeled terminal fields. The tissue was incubated immediately for 2.5 h in phosphate-buffered saline (PBS) containing 1:100 avidin-biotin (Vector Labs) and 0.05% Triton X-100, followed by a cobalt intensified diaminobenzidine/glucose oxidase reaction as described previously (Adams 1981; Kevetter and Perachio 1986). The tissue then was dehydrated through ethanol (50, 70, 95, and 100%) to 100% propylene oxide and embedded in EPON resin. This procedure was performed on each animal to preserve the sensory neuroepithelium for subsequent anatomic studies. After the perfusion, the brain was dissected out of the calvarium and immersed in a solution of 25% sucrose in fixative overnight. The tissue then was embedded in gelatin/albumin, cut on a cryostat to 40-μm-thick sections that were floated into phosphate buffer (0.1 M), and incubated after the above histochemical protocol. Sections then were rinsed in phosphate buffer (0.1 M), mounted on subbed slides, and coverslipped. In six of these animals, the contralateral superior and inferior vestibular ganglia were collected with their intact ampullary nerves and end organs from the temporal bone. This was done to allow visualization of the vestibular efferent axons as they passed from the nerve, through the ganglia and individual ampullary nerves, on their way to their target end organs.

In eight gerbils, unilateral extracellular injections were made in the contralateral dorsal group e with the selective anterograde tracer biotinylated dextran amine (BDA). A solution of 10% BDA (10,000 MΩ Sigma) in PBS (0.01 M, pH 7.4) was injected extracellularly into the dorsal ipsilateral group e after the above protocol for biocytin. After a survival of 7–14 days, to allow transport of

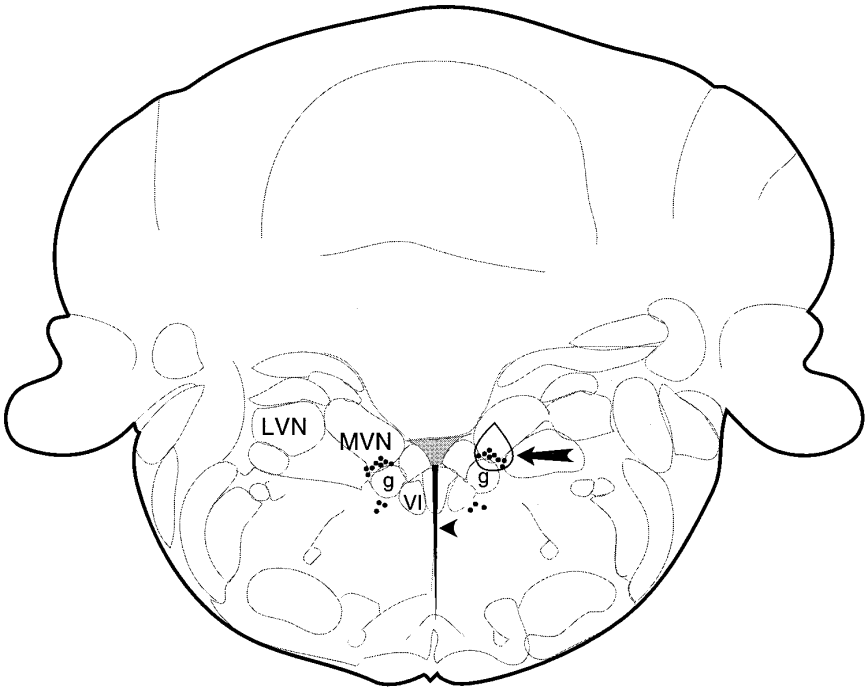

FIG. 1. A line drawing representing a transverse section of the gerbil brain stem showing the site of injection of biocytin or biotinylated dextran amine. Arrow, annulus of tracer spread of a typical ionophoretic injection into the group of efferent neurons (group e) located dorsal and lateral to the genu of the facial nerve. Arrowhead, location and depth of the midline lesion transecting contralaterally projecting efferent axons traveling below the floor of the 4th ventricle. g, genu of the facial nerve; VI, abducens nucleus; MVN, medial vestibular nucleus; LVN, lateral vestibular nucleus.

the label, the animals were anesthetized with urethan (0.7 ml, 500 mg/kg ip) and perfused transcardially with a warmed gerbil Ringer solution followed by a cold solution of fixative containing 4% paraformaldehyde, 0.1 M L-lysine (monochloride), and 0.01 M sodium-m-periodate in 0.1 M PBS (Veenman et al. 1992). The brain stem and the contralateral canal cristae were collected and processed according to the protocol for biocytin above.

The site of the biocytin or BDA injection was examined in all animals to verify that the dorsal cell group of the contralateral group e was the target of the electrode and that the annulus of direct spread of the ejected tracer did not appear to extend ventral to the genu or cross the midline (Fig. 1). Any tissue that did not meet these criteria or had evidence of labeling in the subgenu efferent group was not analyzed. Primary vestibular afferents in the gerbil have not been shown to cross the midline to innervate the contralateral brain stem or sensory neuroepithelium (Kevetter and Perachio 1986). Therefore, a well-localized unilateral injection of label assured that end organs in the contralateral labyrinth contained only fibers of efferent origin and not retrogradely labeled afferent neurons. Additionally, Scarpa's ganglia on the side contralateral to the injection was examined for any labeled cell bodies before any tissue was selected for analysis and reconstruction.

IPSILATERAL BRAIN STEM INJECTIONS. In 12 gerbils, a midline lesion was made in the brain stem to transect the crossed efferent axons 14 days before unilateral extracellular injections of BDA to the dorsal group e. BDA is optimal for ipsilateral injections because it provided a much more selective dark and robust anterograde labeling of even the smallest efferent axons and terminal fields. Any afferent neurons inadvertently labeled presented with a much lighter reaction product, allowing clear distinction between efferent and afferent terminal fields. A 0.6-mm dental burr was used to expose the surface of the cerebellum, and a thin blade with a width of 0.5 mm and a thickness of 50 μm was used to make a cut 7.0 mm deep extending 1.0 mm anterior and 1.0 mm posterior to the anterior-posterior location of the dorsal *group e* neurons. After a 14-day survival, a time adequate to induce degeneration of any contralaterally projecting efferent neurons crossing the midline, unilateral extracellular injections of a solution of 10% BDA were made near the dorsal group e after the above protocol for biocytin. After a survival of 7–14 days, to allow transport of the label, the animals were anesthetized and perfused transcardially with a warmed heparinized saline (10,000 iu/l) followed by a cold solution of fixative containing 4% paraformaldehyde, 0.1 M L-lysine (monochloride), and 0.01 M sodium-m-periodate in 0.1 M PBS (Veenman et al. 1992). The brain stem and the ipsilateral canal cristae were collected and processed according to the protocol for biocytin above. Transverse sections (40 μm) through the brain stem at the level of the genu of the seventh nerve were collected, mounted, and examined to verify the location of the glial scar (Fig. 1) along the midline and to make sure that no labeled axons could be seen crossing the glial scar.

Morphological analysis

TISSUE PREPARATION. Before any tissue was chosen for reconstruction, the vestibular ganglion was examined for any labeled somatae suggestive of the presence of labeled afferent neurons. All embedded end organs chosen to be examined at the light microscopic level were trimmed with a glass knife of any excess embedding material to within ~5–25 μm of the sensory neuroepithelium. The corner of the block then was carefully glued to a glass slide with cyanoacrylate adhesive and bathed in immersion oil. The cristae were oriented to allow optimal reconstruction of the efferent terminal fields. After examination of the tissue in the whole mount, some cristae were photographed and transversely sectioned (5–10 μm). The sections were collected on glass slides, counterstained with toluidine blue, and coverslipped with Permount. Examination of these sections yielded: confirmation of the accuracy of the three-dimensional reconstructions, the point at which the parent fibers penetrated the basement membrane, and the location of the terminal field boutons with respect to the apical and basolateral surfaces of the calyces and type II hair cells.

The vestibular ganglia with intact nerves were prepared and examined in the whole mount for labeled efferent axons. The tissue then was sectioned (5 μm) with glass knives, counterstained with toluidine blue, coverslipped, and examined with a ×40–100 oil objective. The presence of axonal branching and the coursing pattern of labeled fibers were noted. However, no axon counts were made of biocytin or BDA-positive axons.

THREE-DIMENSIONAL RECONSTRUCTION AND ANALYSIS. Three-dimensional (3-D) imaging and morphometry of anterogradely labeled vestibular efferent terminal fields was performed with a Neurolucida imaging system (MicroBrightField). This PC-based system consists of an Olympus (BH-2) microscope with an encoded motorized stage control, 800 × 600 dpi video interface (Video Blaster), and graphics overlay tracing environment (Glaser and Glaser 1990). The sectioned and whole-mounted end organs containing labeled fibers were examined with ×40–100 oil-immersion objectives. Neurons chosen for subsequent 3-D reconstruction and morphological analysis were stained darkly and appeared to contain the tracer label in even the smallest terminal processes. Only those axons were traced from their cut edge at the site of amputation in the ampullary nerve, through the basement membrane, to their terminations in the sensory neuroepithelium. The location and diameters of traced axons, branch points, boutons, and target structures were entered into a Cartesian coordinate system to generate an accurate (±0.5 μm) 3-D graphic image at a final magnification of ×4,500. Morphometric variables of the reconstructions, similar to those used by Brichta and Peterson (1994) to classify afferent terminals in the turtle cristae, were collected and used in a multivariate analysis. Included were *1*) length—the total length summation of all the individual nth order branches contained within the traced efferent neuron's terminal field for the end organ of interest; *2*) order—a measure of the neuron's branching complexity; *3*) endings—a measure of all bouton terminals except those en passant; *4*) number of boutons—a count of all identified varicosities or bouton-like swellings of the axon, either boutons en-passant or boutons termineaux; *5*) linear density of boutons—an average of the total number of boutons per linear micron of the axon's terminal field, calculated by dividing the total bouton count by the summed total of all axon lengths penetrating and traveling within the sensory neuroepithelium; *6*) symmetry of terminal field—a symmetry score assigned for each terminal field in a flattened hemicrista using a method modified from Brichta and Peterson (1994). A circular grid with sectors defined at 45° increments was placed over the centroid of penetration by the parent axon of the flattened terminal field of interest with the axis between 90 and 270° oriented parallel to the longitudinal axis of the crista. The axis values of the grid then were assigned with 0, 90, 180, and 270° aligned with the lateral slope, transverse axis, apex, or planum of the cristae, respectively. A symmetry score ranging from 0.5 (radially symmetrical) to 1.0 (maximum elongation) was obtained by counting the number of boutons in the two opposing quadrants with the most boutons and dividing by the total number of boutons. *7*) Orientation of terminal field—the orientation of the two opposing quadrants with the most boutons. If the two opposing quadrants were aligned with the 90–270° axis of the grid, an orientation score of 1 was assigned to the terminal. If the opposing quadrants aligned with the 0–180° axis, a score of 3 was assigned to the terminal. Scores of 2 or 4 were assigned for orientations aligned 45° off the longitudinal axis toward either the planum or transverse axis, respectively. *8*) Projection—the major direction that the axons of the terminal field tend to ''project'' or travel relative to the centroid of penetration of the basement membrane by parent efferent axons. The hemifield with the most boutons was identified as being localized toward 90° (the transverse axis), 270° (the planum), 180° (the apex), 0° (the lateral slope/periphery), or any of the 45° increments in between. *9*) Location—terminal field location designated as: central, peripheral, or planum (Fig. 2) was modified from that described earlier in chinchilla (Fernandez et al. 1988). Specifically, a neuron with ≥90% of its terminal field confined to the central zone of a hemicrista was identified as a central zone neuron. A neuron with ≥90% of its terminal field confined to the noncentral zone of a hemicrista was identified as a peripheral zone neuron. Although obvious crossing of small higher order terminal collaterals between the central and noncentral zones was rarely observed ($n = 12$), we set the zoning limits at 90% to allow for error in defining boundaries between the zones. Any neuron with a parent axon penetrating the basement membrane in the planum zone and possessing a collateral that crossed the longitudinal axis of the crista was identified as a planum zone neuron (Fig. 2). *10*) Area of innervation—calculated by rotating the Cartesian frame of a reconstructed terminal field until a maximum *X*-*Y* cross-sectional area with minimal *Z* spread was obtained. The coordinate values of all bouton locations then were imported into a software package (Mathematica, Wolfram Research) where a planar plot of the data was generated. A matrix (1 μm^2 grid) incorporating the planar plot was generated. The matrix was examined, and for each individual bouton point, an ''exterior'' point was assigned. These points were placed in the matrix, a standardized 2 μm away from that bouton point in either the *X* or *Y* direction perceived as being located outside of, or not belonging to the neuron's terminal field. Next, points representing boutons ''within'' the terminal field and points located ''exterior'' to the terminal field, were assigned arbitrary values of one or five, respectively. A value of zero was assigned to all remaining unknown points in the matrix. The matrix then was imported into another software package (Transform, Spyglass) where the data were transformed using a filling algorithm (Kriging) to estimate

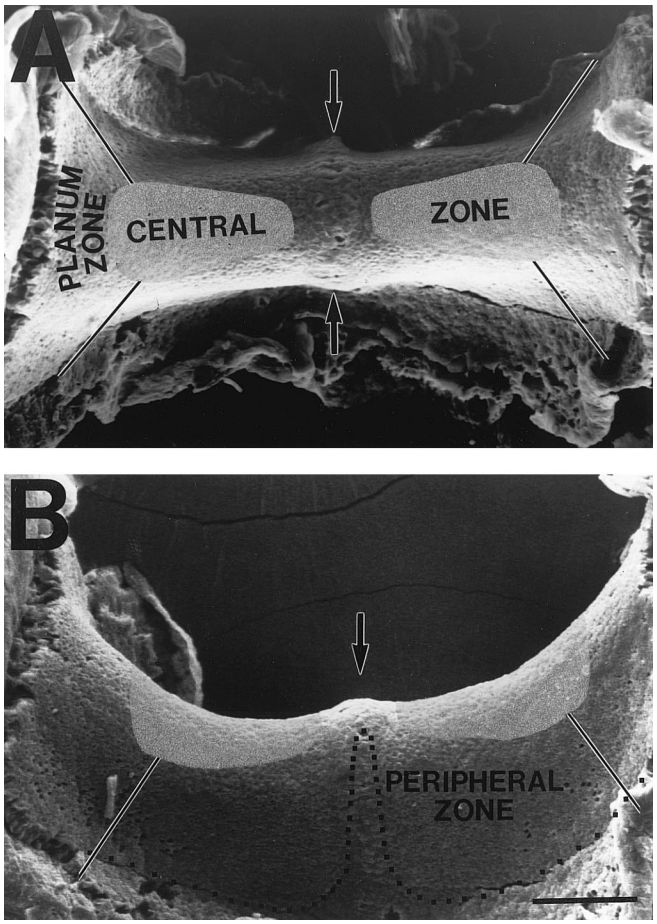

FIG. 2. Zones of the crista ampullares. Top view (*A*) and side view (*B*) of an anterior canal crista with the cupula removed and the membranous canal dissected away. To best describe the efferent innervation of the sensory neuroepithelium, 3 zones have been defined. Central zones, shaded light gray and located in the apex of each hemicrista, are separated by the eminentia cruciata, a hair cell free area (→). Peripheral zones are located on the utriculo-petal and utriculo-fugal sides of the sensory neuroepithelium between the central zone and the floor of the ampulla. Planum zones extend from the central and peripheral zones to the canal walls. For descriptive purposes, the transverse axis is oriented between the 2 arrows in *A.* Scale bar = 100 μm.

TABLE 1. *Morphological variables of efferent terminal fields*

Variable X	Central Zone	Peripheral Zone	Planum Zone
Total axon length, μm	883.0 ± 134.4	1,341.2 ± 142.6	3,174.8 ± 366.1
Number of boutons	85.3 ± 13.1	165.1 ± 17.9	345.7 ± 51.2
Linear bouton density	0.09 ± 0.01	0.13 ± 0.01	0.11 ± 0.01
Number of terminal endings	27.8 ± 5.6	33.3 ± 3.5	71.0 ± 10.2
Order	12.4 ± 2.1	12.1 ± 0.7	20.7 ± 1.5
Innervation area, μm^2	774.1 ± 125.3	1,644.1 ± 145.9	3,303.9 ± 446.0

Values are means ± SE; number of fields for Central zone was 8, for Peripheral zone was 22, and for Planum zone was 9. Statistical comparisons across the three zones are described in text.

the area of innervation (Davis 1973; Isaaks and Mohan-Srivaslava 1989).

CORRECTIONS TO THE PRIMARY DATA. The terminal field innervation area and length data obtained from the horizontal, anterior, and posterior cristae ampullares, were normalized to account for any differential shrinkage between the embedded tissue. The sensory neuroepithelia of the hemicristae were outlined (Neurolucida imaging system) and areas calculated (Transform, Spyglass). Normalization factors (A_{avg}/A_{canal}) and $(A_{avg}/A_{canal})^{0.5}$, where A is area, were applied to all terminal field area and axon length data respectively. A_{avg} is the mean area of all cristae containing reconstructed efferent axons and A_{canal} is the area of the individual crista.

STATISTICAL ANALYSIS. A PC-based statistical package (STATISTICA, StatSoft) was used to calculate Mann-Whitney *U*-tests for the variables listed in Table 1 and simple linear correlations (Pearson r) on the terminal field data (Table 2). Principal components and discriminant function analysis (Tables 3 and 4) were used to determine if vestibular efferent terminal fields can be separated into statistically distinct subpopulations and to determine which morphological variables are the best predictors for discriminating between types. Values will be presented as means ± SD unless otherwise indicated.

RESULTS

Anatomy of the crista ampullares

The cristae ampullares in the gerbil semicircular canals are saddle shaped structures (Fig. 2). They possess a longitudinal axis measuring 682 ± 54 μm ($n = 28$) lying perpendicular to the plane of the semicircular canal. The short or transverse axis (Fig. 2) of the saddle lies parallel to endolymph flow and measures 98 ± 36 μm, ($n = 28$). The width of the crista increases at each end of the saddle near the canal wall to 208 ± 56 μm, ($n = 28$) to form the planum, which lies adjacent to the planum semilunatum (Friedmann and Ballantyne 1984). Our observations of the gerbil sensory neuroepithelium indicate that, similar to that of cat and rat (Igarashi and Yoshinobu 1966; Lewis et al. 1985), each vertical canal crista contains two patches of clearly demarcated sensory neuroepithelium called hemicristae. These hemicristae are oriented with their bases toward the junction of the planum semilunatum and canalicular walls, and their apices opposed at the center of the canal. A transverse ridge of specialized nonsensory epithelial cells referred to as the eminentia cruciata (Friedmann and Ballantyne 1984) (Fig. 2) separates them. Although this structure is not present in the gerbil horizontal crista, we have observed very few efferent terminals in the sector of the horizontal canal crista that corresponds to the region of the eminentia cruciata of the vertical canals.

The sensory neuroepithelia of the cristae may be divided into central, intermediate, and peripheral zones of equal areas distinguished by the density of hair cells and the morphology of afferent calyx endings (Fernandez et al. 1988; Lindeman 1969). In gerbil, the large vestibular efferent terminal fields very often cross the classic ''afferent'' intermediate and peripheral zones mentioned above (Figs. 3–5). Therefore, for optimal description of regional patterns of ''efferent'' innervation, we elected to divide each hemicrista into three efferent zones: the central zone, occupying the apex region excluding that part which extends into the planum region, the peripheral zone, consisting of the merged intermediate and peripheral zones (Fernandez et al. 1988), and the planum zone, beginning at the distal border of the central zone's long axis and extending into the area where the sensory neuroepithelium merges with planum semilunatum and membranous canal wall. This region encompasses that part of the efferent peripheral zone that would normally extend into the planum of the crista (Fig. 2). The regions distal

TABLE 2. *Correlation matrix: terminal fields of central, peripheral, and planum efferent neurons*

Efferent Terminal Fields	Total Axon Length, μm	Number of Boutons	Linear Bouton Density	Number of Terminal Endings	Order	Innervation Area, μm^2	Symmetry	Orientation	Projection
Total axon length, μm									
Number of boutons	0.93*								
Linear bouton density	−0.01	0.31							
Number of terminal endings	0.93*	0.93*	0.14						
Order	0.83*	0.79*	−0.01	0.90*					
Innervation area, μm^2	0.93*	0.91*	0.11	0.86*	0.74*				
Symmetry	0.34†	0.29	−0.20	0.34†	0.33†	0.29			
Orientation	−0.00	0.07	0.30	−0.08	−0.20	0.10	−0.18		
Projection	0.19	−0.07	0.27	−0.15	−0.24	−0.06	−0.37†	0.31†	

* $P < 0.001$. † $P < 0.05$.

and proximal to the utricle, for the peripheral and planum zones, appear symmetrical. As the peripheral zone approaches the transverse axis, it narrows as it follows the eminentia cruciata, up into the apex of the crista at the center of the canal, making the central zones appear discontinuous between the two hemicrista (Fig. 2*B*). The eminentia is absent in the horizontal crista, but dense labeling of efferent and afferent terminals often suggests a similar division of the neuroepithelium into two hemicristae. The mean estimated total sensory neuroepithelial area for the cristae ampullares containing reconstructed efferent terminal fields was 0.129 ± 0.011 mm^2.

Morphometry of the horizontal, anterior, and posterior ampullary nerves

The superior and inferior divisions of Scarpa's ganglion and their intact vestibular and ampullary nerves were examined in four animals after biocytin injection into the contralateral dorsal group e. Multiple labeled efferent axons were identified coursing through the ganglia, vestibular nerve, and ampullary nerves of all cristae. All labeled axons were examined along their path in the nerve and ganglia for signs of collaterals and subsequent innervation of multiple end organs. No branching fibers were identified in the tissue examined with the exception of subepithelial bifurcations <200 μm from the neuroepithelium of the cristae. This is not in agreement with previous evidence of collateralization in the nerve (Gacek 1974) and may very well be due to inadequate penetration of chromagen into the whole-mount nerve and ganglia or suggests efferent collateralization more proximal in the brain stem. No bouton like swellings were identified associated with the labeled efferent axons in either superior or inferior ganglia or the proximal ampullary nerves.

The distal ampullary nerves and end organs of four anterior, two posterior, and four horizontal cristae, containing anterogradely labeled efferent neurons from ipsilateral group e BDA injections, were examined. In 6 of the 10 specimens, there were also multiple retrogradely labeled afferent neurons present in the amputated ampullary nerves. These fibers were stained lightly in contrast to the darkly stained efferent fibers. The labeled afferent neurons of the ampullary nerve of an individual crista form two bundles on either side of the transverse axis to innervate the two hemicristae. After the ampullary nerve bifurcates to innervate one of the hemicristae, afferent terminals were confined to that hemicrista. The only exceptions were a few ($n = 8$) central zone calyx or dimorph afferent endings of axons that could be seen crossing the transverse axis from the ampullary nerve of one hemicrista to innervate the proximal central zone of the adjacent hemicrista. This was observed in both vertical and horizontal canals. The labeled afferent parent axons in the ampullary nerves always coursed through the stroma in a moderately straight path en route to innervate the hemicristae. This was in stark contrast to the darkly stained anterogradely labeled efferent parent axons, which always displayed a very tortuous course throughout the ampullary root (Fig. 3*A*). It was not until the efferent axons were within <200 μm of the crista that they typically were observed to collateralize (up to a third order) before penetrating the hemicristae. No efferent axons were observed crossing the transverse axis before penetration of the basement membrane.

Low order branches of efferent axons labeled from BDA injections into the ipsilateral or contralateral group e displayed a wide range of diameters before penetration of the basement membrane. Neurons innervating the planum zone possessed the largest ($2-3$ μm) parent axon of any labeled efferent neurons. The intermediate diameters ($0.5-2$ μm) were those neurons innervating the central zone and peripheral zone nearer to the planum. The smallest diameters ($0.2-1$ μm) were consistently those neurons innervating the regions of the peripheral zone closest to the transverse axis.

TABLE 3. *Principal component analysis of efferent neuron terminal fields*

	Principal Component 1	Principal Component 2	Principal Component 3
Total axon length, μm	0.952*	−0.162	0.022
Number of boutons	0.972*	0.019	0.135
Linear bouton density	0.201	0.564	0.398
Number of terminal endings	0.975*	−0.072	−0.043
Order	0.889*	−0.139	−0.218
Innervation area, μm^2	0.928*	−0.061	0.146
Symmetry	0.286	−0.795*	0.123
Orientation	−0.035	0.172	0.924*
Projection	−0.093	0.725*	0.248
Percent variance	51.0	17.3	13.1

* Factor variance > 0.700.

TABLE 4. *Discriminant function analysis of efferent neuron geometry*

Efferent Terminal Fields	Discriminant Function 1	Discriminant Function 2
Total axon length, μm	1.45	−1.465
Number of boutons	−1.158	0.134
Linear bouton density	0.887	−0.248
Number of terminal endings	−1.108	1.305
Order	0.391	−0.695
Innervation area, μm^2	0.533	−0.194
Symmetry	−0.096	0.051
Orientation	0.715	−0.142
Projection	0.74	0.44

Regional distributions of efferent terminals

CONTRALATERALLY PROJECTING NEURONS. Unilateral extracellular injections of the anterograde tracer biocytin ($n = 28$) or biotinylated dextran amine ($n = 8$), were placed into the dorsal group e, labeling efferent axons that were traced across the midline into the contralateral labyrinth. These axons were observed traveling across the midline just ventral to the fourth ventricle. Their course neared and penetrated the ipsilateral group e and facial nerve before joining the vestibular primary afferent neurons forming the root of the eighth nerve. In 22 animals, we obtained successful transport of label into the contralateral labyrinth. A total of 748 labeled axons were identified in the sensory neuroepithelium of 16 anterior, 12 posterior, and 12 horizontal cristae. In all end organs examined, the terminal fields of the efferent axons innervated the peripheral and planum zones of both lateral slopes of the sensory neuroepithelium (Figs. 3 and 4). Of

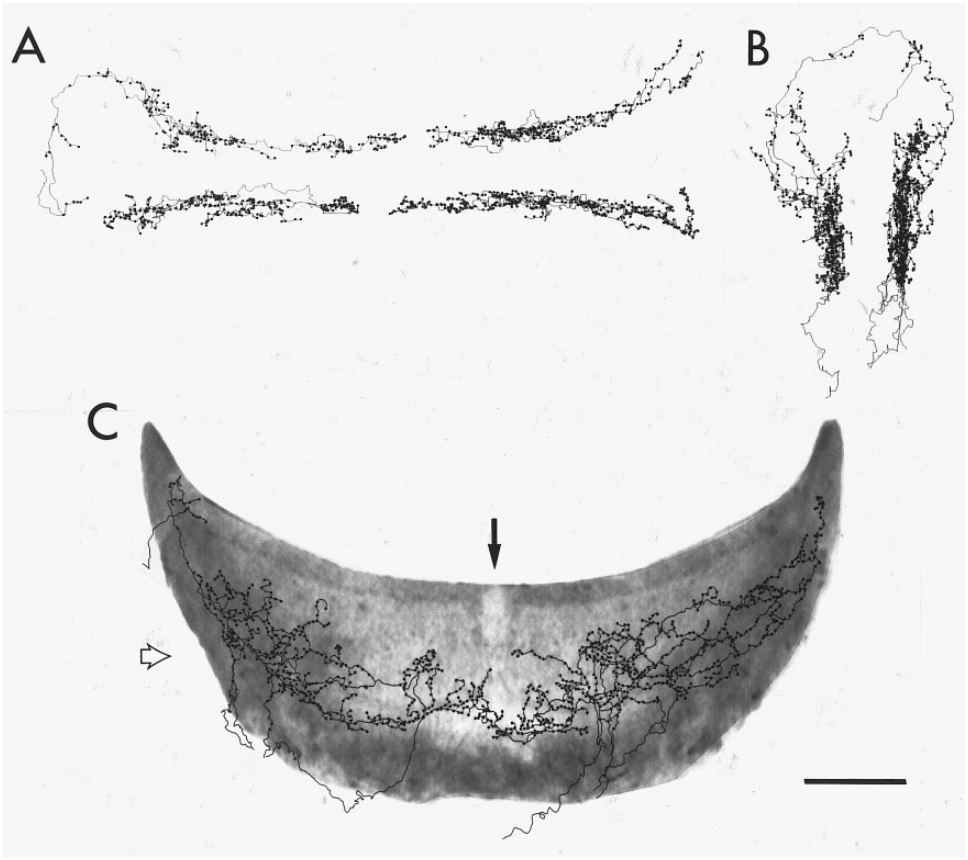

FIG. 3. Reconstruction of the terminal fields of 7 contralaterally projecting efferent neurons innervating the crista ampullares of a horizontal semicircular canal. Terminal fields of these neurons, labeled with extracellular injections of biocytin into the contralateral group e, were restricted to the peripheral and planum zones of the sensory neuroepithelium. In this and all contralateral cristae from this animal, the central zone was absent of any innervation. Note many of the neurons (e.g., *second* from the *left*) bifurcate below the sensory neuroepithelium. *A*: top view. *B*: end view along the longitudinal axis. *C*: side view along the transverse axis. Filled arrow, location of the transverse axis. Open arrow, view in *B*. Scale bar = 100 μm.

those neurons that innervated the noncentral zones of the cristae, 72% (539/748) (range 2–42) innervated the peripheral zone and 28% (209/748) (range 1–13) innervated the planum zone. Peripheral efferents, innervating a particular hemicrista, never were observed to cross the longitudinal axis of the hemicrista either by traveling up and over the apex or collateralizing in the amputated ampullary nerve. On penetrating the basement membrane of the sensory neuroepithelium, only higher order collaterals from a few peripheral zone efferents were observed to crossed the transverse axis of the crista. Those fibers followed the border of the eminentia cruciata up to the apex of the sensory neuroepithelium and into the peripheral zone of the adjacent hemicrista (Fig. 4). Planum zone efferents innervated one hemicrista and were not observed to cross the transverse axis. These typically very large terminal fields always possessed one major projection coursing down the lateral slopes of the planum and peripheral zones ipsilateral to the side of the long axis where the parent axon penetrated the basement membrane of the planum. At least one major projection always was identified traveling up and over the planum, crossing the longitudinal axis of the crista, and continuing back toward the transverse axis to innervate the contralateral slopes of the hemicrista. The central zones of the contralateral cristae were devoid of any terminal field innervation in 18 of 22 (82%) animals (Figs. 3–5). In four animals, we observed the presence of a small number of labeled efferent terminal fields ($n = 26$) in the central zones of two anterior, three posterior, and three horizontal canal cristae. This labeling was in addition to the characteristic peripheral and planum zone labeling. The overall patterns of innervation observed for the peripheral and planum terminal fields did not vary significantly between the anterior, posterior, or horizontal canals.

IPSILATERALLY PROJECTING NEURONS. In 9 of 12 animals, after complete midline brain stem lesions of the contralaterally projecting efferent axons, successful transport of BDA into the ipsilateral labyrinth was obtained. A total of 259 labeled parent axons were identified in the amputated roots of seven anterior, seven posterior, and seven horizontal cristae. Three anterior, three posterior, and three horizontal canal cristae in five different animals contained 62 efferent terminal fields (range 4–10) restricted to the central zones of the hemicristae. Individual central zone terminal fields cross the longitudinal axis but were not observed to innervate the adjacent planum zone or project across the transverse axis to the other hemicrista (Fig. 6). Only rarely did we see a central zone collateral ($n = 2$) extending minimally into the slopes of the peripheral zones. Four anterior, four horizontal, and four posterior canal cristae contained a total of 197 (range 5–26) efferent terminal fields innervating the central, in addition to the peripheral and planum, zones. The regional distributions of the central zone terminal fields, 35% (68 of 197; range 3–10), were similar to those described earlier. The peripheral, 53% (105 of 197; range 0–19), and planum, 12% (24 of 197; range 0–3), zone terminal fields were distributed regionally similar to those labeled in contralateral group e injections. The general patterns of innervation observed did not vary significantly between the anterior, posterior, or horizontal canals.

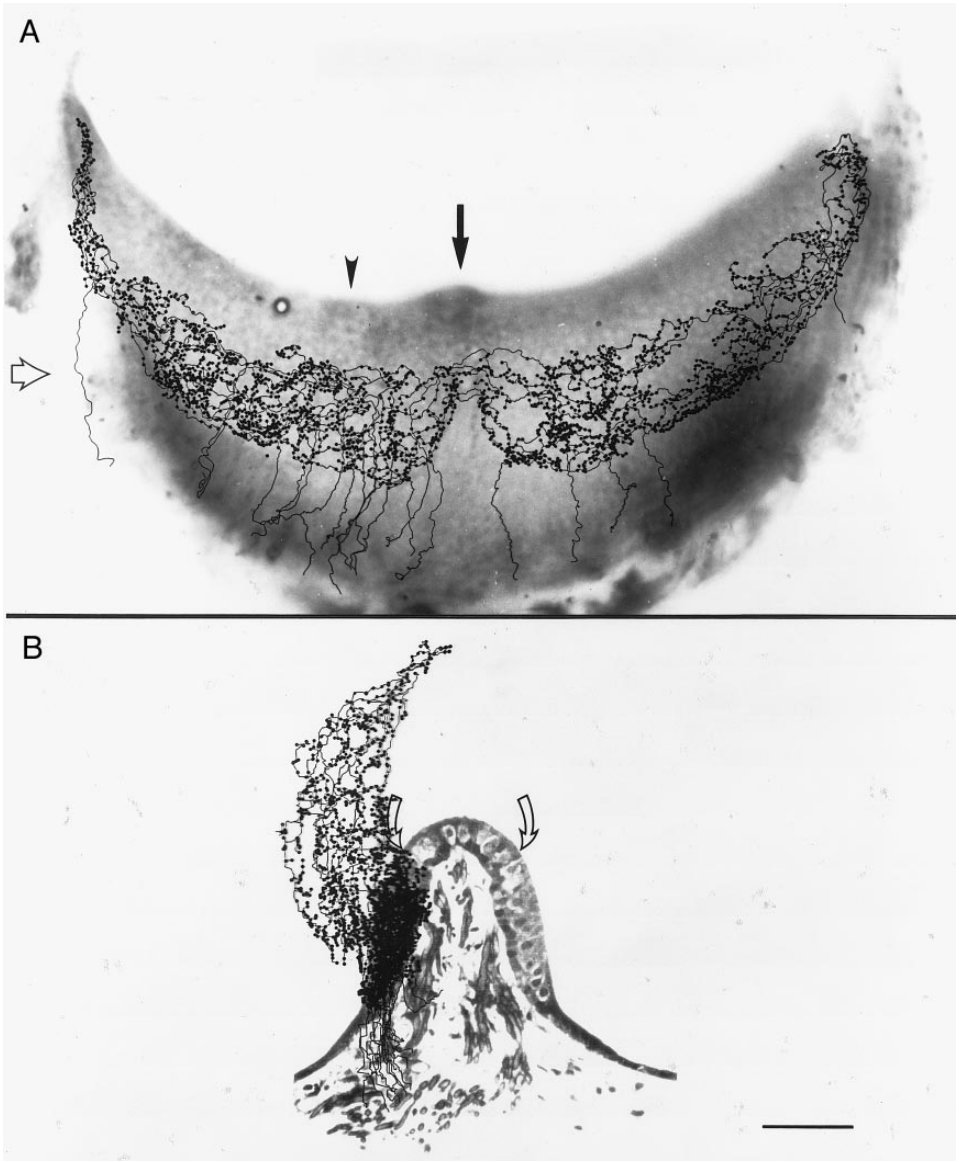

FIG. 4. Reconstruction of the terminal fields of 16 contralaterally projecting efferent neurons innervating the crista ampullares of a posterior semicircular canal. Terminal fields of these neurons labeled with extracellular injections of biocytin into the contralateral group e were restricted to the peripheral and planum zones of the sensory neuroepithelium. Central zone was absent of any innervation. Parent axons of many of these terminal fields bifurcated well below the sensory neuroepithelium (e.g., fifth from left). *A*: side view along the transverse axis. *B*: end view along the longitudinal axis with all the reconstructed terminal fields collapsed to 1 side and overlaid on a transverse section taken at the location indicated by the arrow head in *A*. Filled arrow in *A* points to the eminentia cruciata and open arrow in *A* indicates view in *B*. Arrows in *B* bracket the central zone in the apex of the crista. Scale bar = 70 μm.

Structure of efferent terminal fields

We reconstructed and analyzed a sample population of labeled terminal fields in an attempt to identify which morphological characteristics distinguish neurons innervating the central, peripheral, and planum zones of the semicircular canal cristae.

CONTRALATERALLY PROJECTING AXONS. The horizontal, anterior, and posterior canal cristae from three animals receiving an extracellular injection of biocytin into the contralateral dorsal group e were chosen for reconstruction because of the excellent preservation of all of the canal tissue, the dark and complete labeling of the efferent terminal fields, and the sparse number of labeled axons allowing accurate tracings and 3-D reconstructions. From a single animal, the horizontal crista contained 7 (Fig. 3), the anterior 3, and the posterior 16 (Fig. 4) labeled neurons. Eight additional terminal fields were selected in the anterior ($n = 5$) and horizontal ($n = 1$) cristae of a second and the posterior ($n = 2$) crista of a third animal. These neurons all terminated with numerous en passant and fewer terminal bouton-like swellings in the peripheral ($n = 25$, 73%) and planum ($n = 9$, 27%) zones of the sensory neuroepithelium of both hemicristae.

Peripheral and planum terminal fields displayed a relatively high degree of asymmetry (0.71 ± 0.09 and 0.82 ± 0.10 symmetry ratios, respectively), with the long axis of the terminal fields typically oriented at an angle of $\pm 45°$ to the longitudinal axis of the crista (Fig. 8*B*). Planum neurons predominately (88%) projected toward the transverse axis, whereas peripheral neurons predominately (81%) projected toward the planum of the crista. Planum neurons typically had the largest innervation areas of any efferent neuron. Peripheral neurons displayed a wide range of innervation areas from small to large moving from the transverse axis toward the planum of the crista. Peripheral terminal fields possessed smaller mean total axon length, fewer boutons and terminal endings, lower order, and smaller innervation area compared with planum terminal fields (Mann-Whitney *U*-test, $P < 0.05$, Table 1). These descriptive variables all were significantly ($P < 0.001$) intercorrelated (Table 2) and had a linear relationship to innervation area (Fig. 7, *A–D*). Although there was a slight tendency for linear bouton

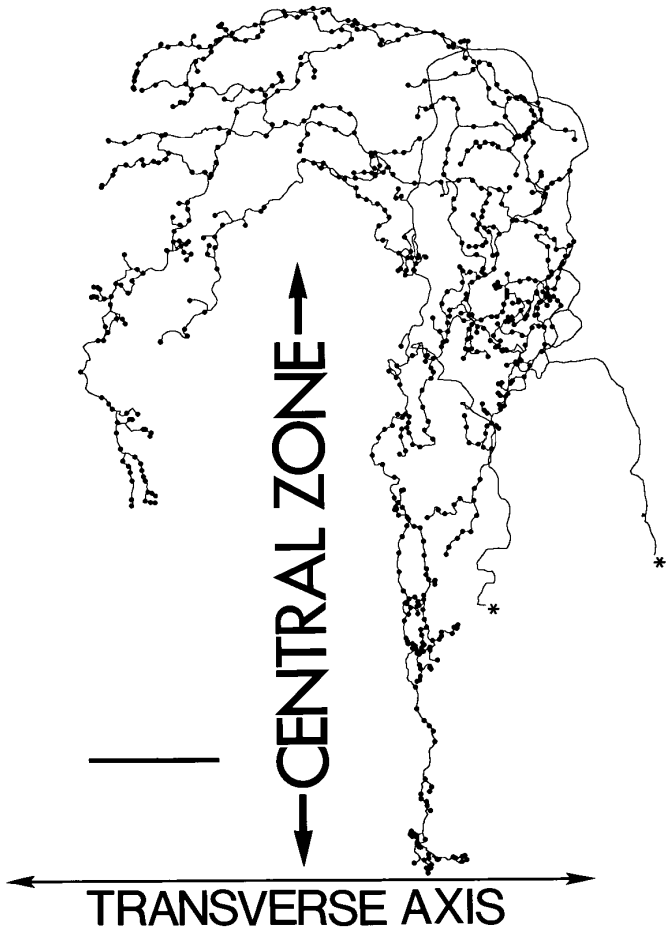

FIG. 5. Top view of 2 planum-type efferent terminal fields innervating the hemicrista of an anterior semicircular canal. Note how the central zone of the sensory neuroepithelium is devoid of terminals. Scale bar = 50 μm.

density to increase as the location of any given terminal field approached the planum, the difference was not significant. Three of the 34 reconstructed neurons in the canal tissue were not used for morphological analysis (see following text) due to incomplete filling of a portion of the smaller preterminal and terminal axons.

IPSILATERALLY PROJECTING AXONS. The posterior crista from an animal receiving an extracellular injection of biotinylated dextran amine into the ipsilateral dorsal group e was chosen for reconstruction. The crista contained seven labeled neurons ending in a spray of bouton en passant and fewer terminal bouton swellings restricted to the central zone of the neuroepithelium of both hemicristae (Fig. 6). An additional terminal field from the horizontal crista of a second animal also was reconstructed. Qualitatively, all the terminal fields were small, asymmetric, and often had tight bouton sprays around the base, body, and neck of afferent calyces. Central terminal fields possess smaller mean total axon length, fewer boutons and terminal endings, lower order, and smaller innervation area compared with planum terminal fields, but fewer boutons, smaller linear bouton density and innervation areas compared with peripheral terminal fields (Mann-Whitney U test, $P < 0.05$, Table 1). With the exception of linear bouton density, all the above descriptive variables had significant ($P < 0.001$) intercorrelations (Table 2). Total axon length, number of terminal endings, number of boutons, and linear bouton density all increase with innervation area and display a linear regression fit with a positive slope (Fig. 7, A–C). Central terminal fields displayed a high degree of asymmetry (0.79 ± 0.17), were oriented along the longitudinal axis, and predominately (88%) projected toward the transverse axis of the crista (Figs. 6 and 8B).

Multivariate analysis

SUBPOPULATIONS OF VESTIBULAR EFFERENT NEURONS. We have identified three possible subpopulations of efferent neurons innervating the central, peripheral, and planum zones of the crista sensory neuroepithelium. To determine if structural differences, independent of location, exist among the terminal fields in these three zones, we performed principal components and discriminant function analysis on the measures of morphological variables.

Principal components analysis revealed that 81.4% of the total variance observed among the population of reconstructed efferent neurons can be attributed to the first three principal components (Table 3). The first component accounts for 51.0% of the total variance. That component is weighted heavily toward the variables describing the morphological characteristics of the efferent terminal fields: axon length (0.952), total boutons (0.972), terminal endings (0.975), order (0.889), and innervation area (0.928). The second principal component accounting for 17.3% of the total variance, is weighted heavily toward symmetry (-0.795) and projection (0.725) of the terminal field in the sensory neuroepithelium. The third principal component, accounting for 13.1% of the total variance, is weighted most heavily toward orientation (0.924). Three groups of efferent neurons are identified when plotting the Factors derived from the first three principal components (Fig. 9, Factors 1–3). The smallest group containing 8, the intermediate group containing 9, and the largest group containing 22 efferent terminal fields represent those neurons innervating the central, planum, and peripheral zones, respectively.

Discriminant function analysis subsequently was performed on the data, resulting in two canonical discriminant functions, each statistically significant ($P < 0.001$) and correctly classifying 38/39 (97%) of the reconstructed efferent neurons. The first discriminant function is weighted most heavily by the variables: total axon length, number of boutons, terminal endings, linear bouton density, terminal endings, and orientation. The second discriminant function is characterized predominately by the variables: total axon length, terminal endings, and order (Table 4). The scatter plot (Fig. 8A) of the canonical scores for pairs of discriminant functions (canonical roots) illustrates the ability of the first discriminant function to discriminate fairly well among the three types of efferent neurons, whereas the second distinguishes mostly between the central and noncentral types. To summarize the findings, it is suggested by our principal components and discriminant function analyses, that three types of structurally distinct efferent neurons may coexist within the sensory neuroepithelium of the crista ampullares.

DISCUSSION

The present study presents evidence for a geometric arrangement of vestibular efferent projections to the sensory

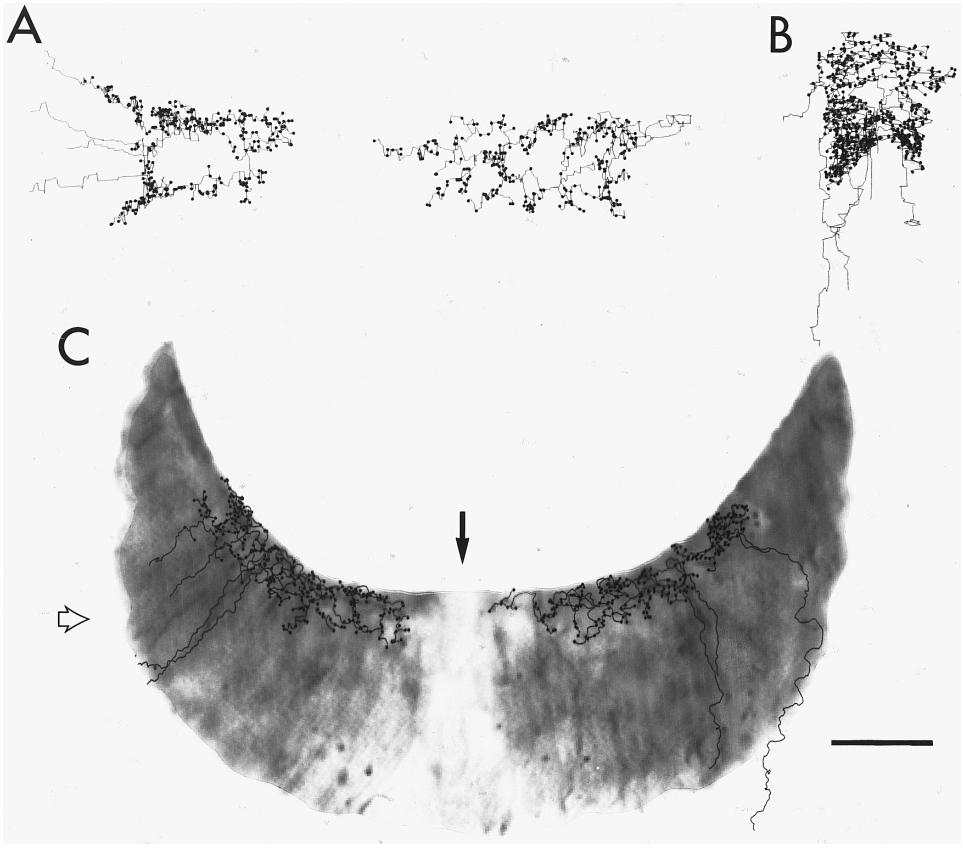

FIG. 6. Reconstruction of the terminal fields of 7 ipsilaterally projecting efferent neurons innervating the crista ampullares of a posterior semicircular canal. Terminal fields of these neurons labeled with extracellular injections of biocytin into the ipsilateral group e were restricted to the central zones of the sensory neuroepithelium. Peripheral and planum zones were absent of any innervation. *A*: top view. *B*: end view along the longitudinal axis. *C*: side view along the transverse axis. Filled arrow, location of the eminentia cruciata. Open arrow, view in *B*. Scale bar = 100 μm.

neuroepithelium of the cristae that is topographic. We describe a relationship between the brain stem location of the cell bodies of origin for the efferent system and the region of the sensory surface that their axons innervate. In addition, evidence is presented that at least three classes of efferent terminal fields can be distinguished on the basis of their areas of innervation, number of bouton endings, axonal lengths, etc. These data suggest a structural organization of efferent innervation patterns that may relate to their modes of influencing afferent background discharge and dynamic responses.

Comparison of vestibular and cochlear efferent innervation of the inner ear

The regional differences in the sites of terminal fields of ipsilaterally versus contralaterally projecting vestibular efferents may be compared with efferent innervation of the mammalian cochlea. The efferent innervation of the cochlea derives from two sources in the superior olivary complex. The unmyelinated lateral olivocochlear (LOC) neurons, staining immunopositive for glutamic acid decarboxylase (GAD) or choline acetyltransferase and CGRP in rat (Vetter et al. 1991) and selectively uptaking D-aspartate in gerbil (Ryan et al. 1987), project predominately to the ipsilateral cochlea. The medial olivocochlear neurons (MOC) predominately project to the contralateral cochlea. They stain immunopositive for ChAT, negative for CGRP (Vetter et al. 1991), and in gerbil (but not rat) selectively uptake GABA (Ryan et al. 1987, 1992; Schwartz and Ryan 1986). Both LOC and MOC neurons appear to be morphologically and spatially heterogeneous in their brain stem location and patterns of innervation of the cochlea. In cat (Guinan et al. 1983, 1984), LOC efferents innervate the entire cochlea with more medially located somatae projecting predominately to the base of the ipsilateral cochlea. All contralateral LOC projections predominately innervate the apex of the cochlea. The MOC efferents project mainly to the middle and basal regions of both cochleas. Contralateral projections are concentrated more in the basal cochlea than those ipsilateral. Also, the more dorsal regions of the MOC-zone project most heavily to the basal cochleas, whereas ventral regions project predominately to the apex. Peripheral labeling of the cochlea demonstrates patterns of regional innervation with the outer hair cells of the basal cochlea contacted by terminals that are immunolabeled for ChAT, glutaminase, and aspartate amino-transferase, whereas the apical portion contains terminals for GABA and glutamic acid decarboxylase (Altschuler and Fex 1986). In rat, GAD or CGRP immunopositive LOC terminals are located under inner hair cells the entire length of the cochlea. Additionally, GAD or CGRP positive LOC terminals make contact with outer hair cells in the apex or apical two-thirds of the cochlea (Vetter et al. 1991). In gerbil (Ryan et al. 1992), GABA uptake and selective retrograde transport of nipecotic acid suggests that MOC neurons project beneath 50% of the inner hair cells and 100% of the outer hair cells. Additionally a small number (average of 5.4%) of individual olivocochlear neurons have been shown to project to both cochleas in mammals (Robertson et al. 1987a,b).

The most obvious parallels between the mammalian vestibular and cochlear system are that they both have two types of hair cells, type I and II or inner and outer, respectively. The type II and outer hair cells make direct contact with

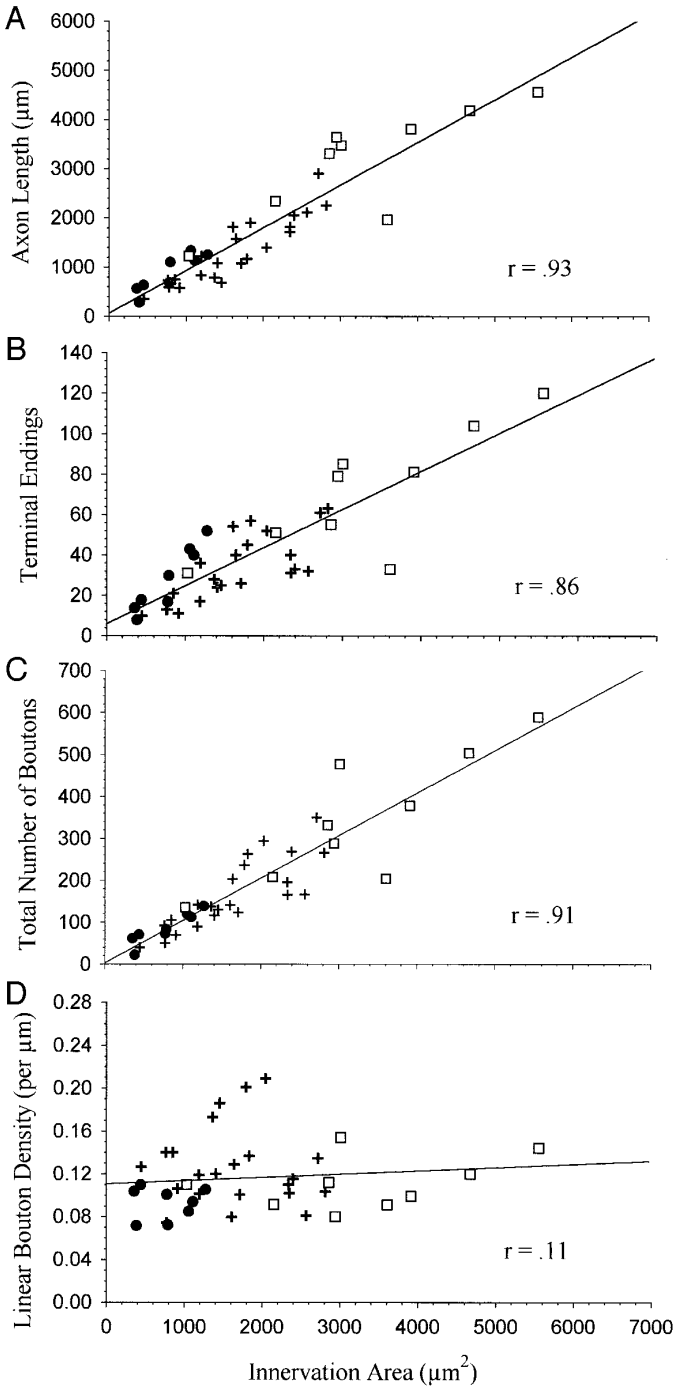

FIG. 7. Relationship between innervation area of efferent terminal fields and morphological characteristics. As innervation area increases, the number of terminal endings (*A*), axon length (*B*), and total number of boutons (*C*) increases ($P < 0.001$). Linear bouton density does not change appreciably as innervation area increases ($P > 0.05$). Regression lines are combined for all 3 types of efferent terminal fields. Filled circle, central zone efferents; plus sign, peripheral zone efferents; open square, planum zone efferents.

both afferent and efferent terminals. Type I and inner hair cells make contact only with afferent terminals, whereas efferent terminals contact the postsynaptic calyx ending or afferent axon beneath those hair cells, respectively (Guinan 1996). The comparison between vestibular and cochlear efferents appears to lie in the segregation of ipsilaterally, contralaterally, and bilaterally projecting types. In the vestibular sensory neuroepithelium, the preponderance of histochemical evidence does not suggest a discrete regional distribution in immunoreactivity for putative neurotransmitters or peptides substances. We previously reported the coexistence of ChAT and CGRP in the gerbil efferent neurons (Perachio and Kevetter 1989). All retrogradely labeled vestibular efferent cells in the dorsal group e appear to be immunopositive for both substances. If specialized neurochemical distribution does exist among vestibular efferent neurons, we would propose that they may reflect the two major populations derived from ipsilateral and contralateral efferent cell groups that respectively innervate the most central versus the peripheral and planar regions of the cristae.

Differential efferent innervation of the crista

The distribution of hair cells in the mammalian cristae have been described most completely in recent studies on the chinchilla and squirrel monkey (Fernandez et al. 1995; Goldberg et al. 1990). Some significant species differences exist regarding the ratio of type I versus type II hair cells and in the relative percentages among the types of afferent terminals that innervate them. However, consistent findings indicate that calyx-only afferents innervate type I hair cells, whereas bouton-only endings are found only on type II hair cells. Respectively, these two types of terminals are distributed spatially predominantly to the central and peripheral zones of the cristae. The remainder (and the majority) of hair cells are innervated by afferent terminals that are dimorphic, combining both calyx and bouton endings. Although data on hair cells and afferent terminal morphology are not available for the gerbil, findings from studies on such disparate mammalian species such as the chinchilla and squirrel monkeys suggest a degree of conservation of morphological organization, so that the central zone of the apex of the cristae is composed of both type I and type II hair cells that are innervated by calyx-only or dimorphic endings. Generalizing this structural arrangement to the gerbil cristae, the ipsilateral efferent innervation of the central zone must project to this mixed population of afferent neurons. Contralaterally projecting efferents by logical extension would provide innervation to the peripheral and planar zones overlying the area associated with dimorphic and bouton-only afferent terminals and relatively fewer calyx-only endings.

Functional considerations

Recent studies have provided some evidence of a structural/functional relationship between the morphology and/or location of afferent terminals and their physiological properties. The latter include measures of the regularity of their background discharge rate and their dynamic responses to either galvanic stimulation of the labyrinth or head rotation. Baird et al. (1988) conducted studies involving intraaxonal labeling of bullfrog afferents combined with physiological characterization. More recently, the morphology of squirrel monkey cristae sensory epithelium and primary afferents was examined by Fernandez et al. (1995). In companion studies, Lysakowski et al. (1995) provided physiological data that related to different structural classes of afferents by inferred relationships between their physiological properties and the morphology of their terminals. This set

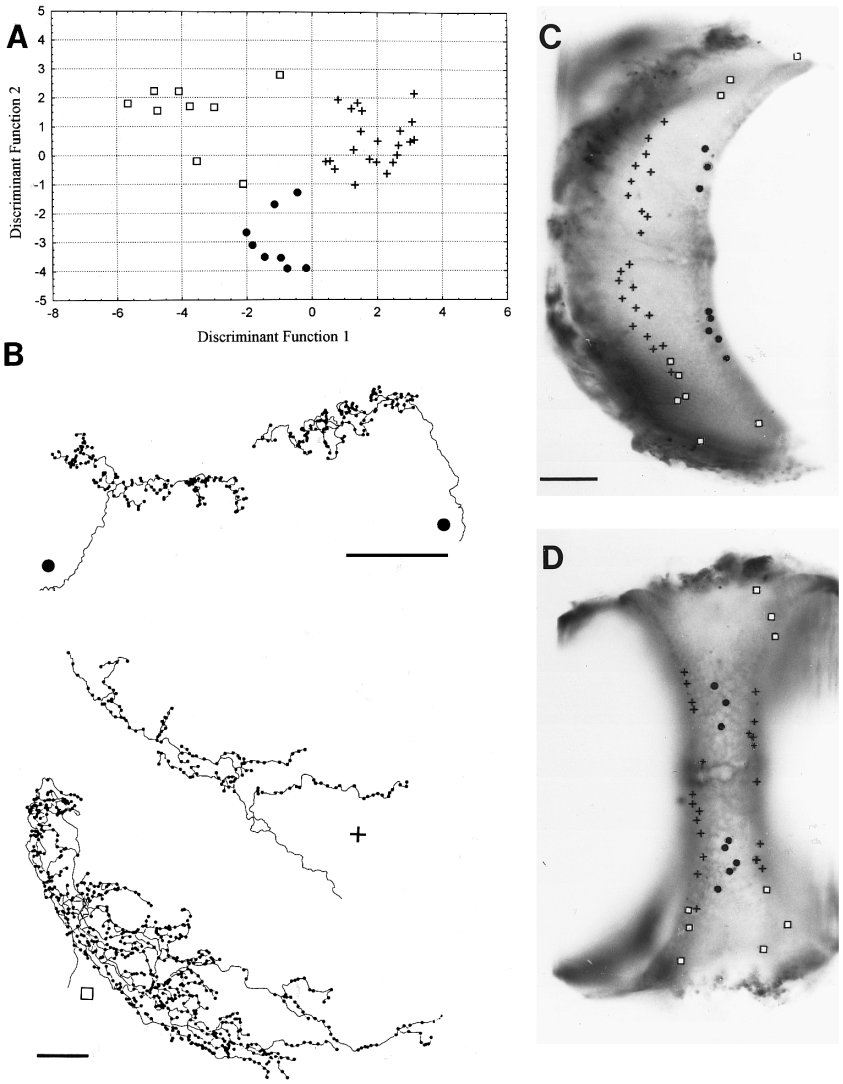

FIG. 8. *A*: scatterplot of the canonical scores for pairs of discriminant functions (canonical roots). Discriminant function analysis of the morphometric variables describing the terminal fields of efferent neurons innervating the cristae ampullares indicates they separate into three subpopulations ($P < 0.001$). Function 1 discriminates well between the central, peripheral, and planum types, whereas function 2 discriminates mostly between central and noncentral types. *B*: reconstructions of efferent terminal fields. Smaller central (●) zone efferents were labeled predominately from tracer injection into the ipsilateral group e, whereas the typically larger peripheral (+) and planum (□) zone efferents were predominately labeled from injections into the contralateral group e (scale bars = 45 μm). Side view (*C*) and top view (*D*) of a composite of all 39 reconstructed efferent terminal fields examined in the multivariate analysis. Entire sensory neuroepithelium is innervated by the 3 types of efferent neurons. Symbols are located at the approximate centroid of the penetration of the parent efferent axons into the sensory neuroepithelium. Scale bar = 90 μm. Symbols are the same as in Fig. 7.

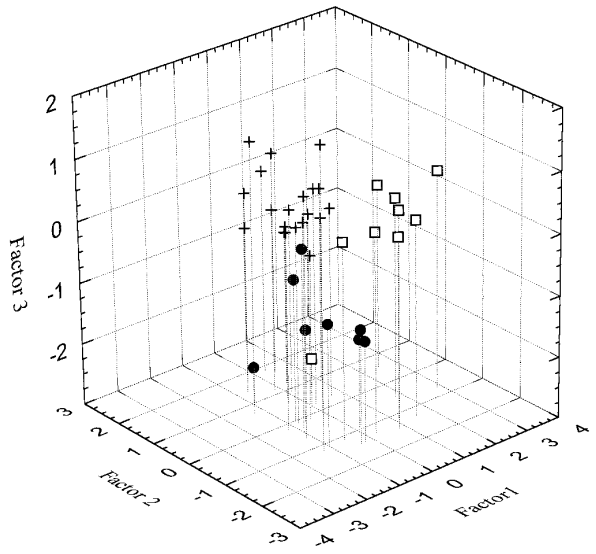

FIG. 9. Principal components analysis of the morphometric variables collected from the terminal fields of efferent neurons innervating the cristae ampullares. Scatterplot of the factors (Factors 1–3) derived from the 1st 3 principal components indicates that the efferent terminal fields separate into 3 subpopulations. Symbols are the same as in Fig. 7.

of studies has provided both direct and indirect evidence linking the anatomic and functional characteristics of primary vestibular afferents.

Dimorphic neurons were found to have the broadest range of functional characteristics. The most regularly firing dimorphic afferent had a low response gain and response phases related to head velocity, whereas the most irregularly discharging units had higher response gains and response phases leading head velocity for rotations at 2 Hz. As a population, calyx afferents had a larger average coefficient of variation (CV = standard deviation of the interspike intervals/mean interspike interval) than dimorphic units. They also were distinctly more sensitive to galvanic stimulation yet were significantly less responsive to head rotation. Moreover, calyx response phase with regard to head velocity was advanced markedly. Bouton units were characterized by the lowest average response gains and phases and their spontaneous discharge rates had the smallest average normalized CV.

Thus the central zone of the cristae is innervated by afferents that differ distinctly in both morphological and functional features from those found predominately in other zones. Intra-axonally labeled dimorphic afferents in the chinchilla, that were located in the central zone, were also those that discharged irregularly and had high response sensitivi-

ties. The central zone calyx units also had highly variable background discharge activity and low sensitivities. How then might the ipsilaterally projecting efferent neurons influence this divergent population of afferents?

In the toadfish (Highstein and Baker 1985) and frog (Caston and Bricout-Berthout 1984), sensory stimulation by visual, auditory, or somatosensory stimuli was found to be effective in elevating efferent background discharge. Comparable information for the responsitivity of mammalian efferent neurons is lacking. Instead, the influence of vestibular activation on primary afferent neurons has been studied in most species by electrical stimulation of the efferent pathways. The most consistent reported findings are that such stimulation produces an elevation of afferent firing rates that is related in magnitude to the afferent discharge variability. Moreover, the magnitude of the response to efferent stimulation also was correlated with the afferent neuron's sensitivity to head rotation. In the squirrel monkey (Goldberg and Fernandez 1980), turtle (Brichta and Goldberg 1996), and toadfish (Boyle and Highstein 1990), irregularly firing high gain units exhibited the largest increase in discharge during efferent stimulation. In contrast, low gain units that were discharging regularly were found to respond minimally to efferent stimulation.

Accepting that those morphological and functional associations between efferent and afferent neurons pertain to the gerbil, it would appear that the ipsilaterally projecting efferents innervate an area that contains the afferent terminals that should exhibit the greatest sensitivity to efferent stimulation. The lowest gain, most regularly discharging afferents would be influenced by the contralaterally projecting efferents. This leaves the calyx units located primarily in the central zones, which have relatively low gain in comparison with the majority of irregularly firing dimorphic afferents, that should be influenced by the ipsilaterally projecting efferents.

The resolution of this seemingly paradoxical arrangement may be understood by consideration of the efferent influences on afferent dynamic responses to natural stimulation. Again, the most definitive studies have been conducted on squirrel monkey and toadfish. In contrast to the generally excitatory influences of efferent stimulation on afferent discharge rate, the rotational gains for the responses of sensitive afferents with response phase leads were attenuated during efferent stimulation. It must be noted however that consideration of this effect as a response attenuation should be qualified. As demonstrated by both Goldberg and Fernandez (1980) for the squirrel monkey and by Boyle and Highstein (1990) for the toadfish, in the case of afferents with low background discharge rates, response to head rotation exhibits rectification (silencing or cutoff) during the inhibitory phase of the response. Efferent elevation of the afferent discharge rate results in a continuous modulation of that activity during head rotation, thus increasing response linearity and input signal fidelity. In the case of calyx units that have the most irregular discharge rate and relatively lower gains than dimorphic units of comparable irregularity, one would expect a significant efferent influence on response linearity.

Model of efferent function

The following is a description of a proposed model that suggests a set of functional conditions that may pertain during active head motion. The model is represented schematically in Fig. 10. Assuming that the efferent system acts to modify afferent responses during the active head motion, it is proposed that an efference copy or premotor signal is received as an input by the cells of the dorsal group e. The signal(s) should differ in sign bilaterally to reflect the bilaterally asymmetric activation of neck muscles, as in the example shown in Fig. 10, that results in a volitional leftward head rotation. In addition, the model assumes some degree of vestibular input to the efferent neurons. This assumption is based on ultrastructural evidence in the rat (White 1985) of direct vestibular afferent projections to the dorsal group e. The afferent signal should be excitatory in light of electrophysiological (Doi et al. 1990; Lewis et al. 1989) and histochemical (Dememes et al. 1990) evidence of excitatory amino acid as the putative neurotransmitter in vestibular afferent terminals.

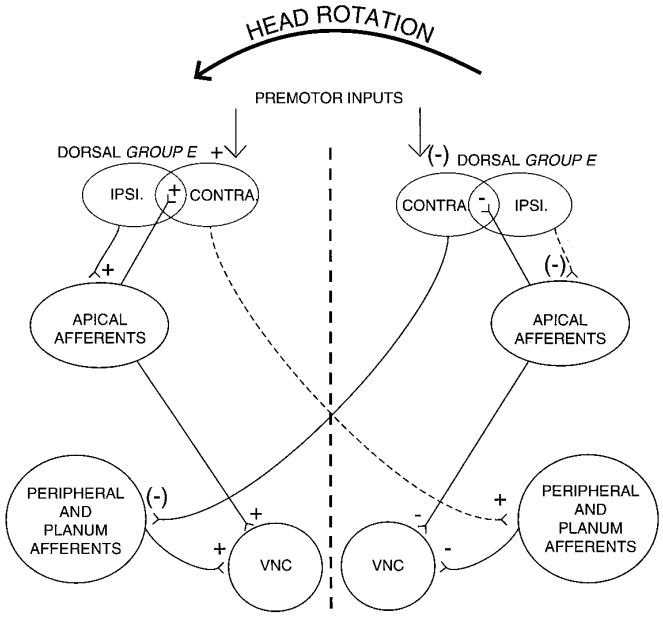

FIG. 10. Schematic illustration of proposed feedback and feed-forward connections between vestibular (dorsal group e) efferents and vestibular afferents of the horizontal semicircular canals. Solid lines, direct or disynaptic connections; dashed lines, opposite connections of separate efferent neurons to the right labyrinth. Plus signs, excitatory input during active leftward head rotation; Minus signs, reduction in excitatory drive; parentheses, no excitation or active inhibition. VNC, vestibular nuclear complex.

During a volitional head turn, it is proposed that the efferent nucleus ipsilateral to the direction of rotation, should be activated immediately before the onset of motion. The contralateral group of neurons should receive no excitatory synaptic stimulus or perhaps may be inhibited actively. The efferent influence on the periphery should reflect the bilateral asymmetric state of the efferent system under these conditions. The functional consequences, in terms of afferent discharge activity and response dynamics, are predicated on existing evidence for the mammalian vestibular system (Baird et al. 1988; Lysakowski et al. 1995; Schneider and Anderson 1976). Before the onset of head rotation, the ipsilateral efferents, projecting to the central zone of the crista, should elevate the activity of calyx and dimorphic afferent fibers that contact hair cells in that region. The former can be expected to exhibit the greatest sensitivity to efferent

input. Subsequently, as head acceleration occurs, the modulation of their elevated activity should be more linear than during passive head motion because response rectification is less likely to occur. The high gain, irregularly discharging dimorphic afferents, innervating the central zone, should similarly exhibit an elevation of their firing rate with comparable improvement in response linearity. The afferents' excitatory input directly affects efferent neurons only on the ipsilateral side. This connection constitutes an ipsilateral closed-loop arrangement. This does not necessarily mean that the feedback signal should reflect the afferent excitatory drive. The contralaterally projecting efferents have open-loop connections with the contralateral afferents. Those efferents, which project to the peripheral and planar zones, should under the same conditions of head acceleration provide no excitatory drive to the labyrinth ipsilateral to the direction of head rotation. Afferents with terminals in the peripheral and planar zones, on the side contralateral to the direction of head motion, should exhibit responses to excitatory efferent inputs. The evidence from combined intraaxonal labeling and physiological characterization in mammalian preparations indicates that dimorphic and bouton-only classes of afferents, the response gains of which range from the intermediate to the lowest afferent gains, innervate the peripheral and planum zones. An elevation in background discharge produced by contralateral efferent excitation should lessen the likelihood of those afferents to exhibit inhibitory cutoff responses to contralateral head acceleration.

The model relates to the efferent system's relationship to the horizontal semicircular canals. The anatomic data we have described for the efferent innervation of the vertical canal cristae is similar to that of the horizontal canal sensory surface. The model as described may be applicable to the bilateral pairs of vertical canals (e.g., left anterior/right posterior vs. right anterior/left posterior) under conditions of oblique or roll plane head tilts. To assess the appropriateness of generalization of the model to vertical canal system, it will be necessary in further studies to assess whether individual efferent neurons project to more than a single crista in the same labyrinth.

In the absence of data on the responses of mammalian efferent neurons to active head motion, simulation of the model is problematic. The evidence provided by Highstein and Baker (1985) from recordings of toadfish efferent responses is supportive of the idea that the efferent system is responsive to premotor inputs that are activated before the initiation of active head motion. Physiological evidence for the bilateral efferent nuclei affecting morphologically and functionally distinct groups of afferents similarly is lacking. Our model and the anatomic findings on which it is based, hopefully, suggest new questions to address concerning the functional role of the vestibular efferent neurons in the regulation of afferent responses.

We thank Drs. Anna Lysakowski and Galen Kaufman for comments made on a previous draft of this paper.

This work was supported in part by National Institute of Deafness and Other Comunications Disorders Grant DC-00385 and National Aeronautics and Space Administration Grant NGT 50748.

Address for reprint requests: A. A. Perachio, Dept. of Otolaryngology, The University of Texas Medical Branch, 301 University Blvd., 7.102 Medical Research Bldg., Galveston, Texas 77555-1063.

Received 28 October 1996; accepted in final form 5 August 1997.

REFERENCES

ADAMS, J. C. Technical considerations on the use of horseradish peroxidase as a neuronal marker. *J Neurosci.* 2: 141–145, 1977.

ADAMS, J. C. Heavy metal intensification of DAB-based HRP reaction product. *J. Histochem. Cytochem.* 29: 775, 1981.

ALTSCHULER, R. AND FEX, J. Efferent neurotransmitters. In: *Neurobiology of Hearing: The Cochlea*, editied by R. Altschuler, D. Hoffman, and R. Bobbin. New York: Raven, 1986, p. 383–396.

BAIRD, R. A., DESMADRYL, G., FERNANDEZ, C., AND GOLDBERG, J. M. The vestibular nerve of the chinchilla. II. Relation between afferent response properties and peripheral innervation patterns in the semicircular canals. *J. Neurophysiol.* 60: 182–203, 1988.

BOYLE, R., CAREY, J. P., AND HIGHSTEIN, S. M. Morphological correlates of response dynamics and efferent stimulation in horizontal semicircular canal afferents of the toadfish, *Opsanus tau*. *J. Neurophysiol.* 66: 1504–1521, 1991.

BOYLE, R. AND HIGHSTEIN, S. M. Efferent vestibular system in the toadfish: action upon horizontal semicircular canal afferents. *J. Neurosci.* 10: 1570–1582, 1990.

BRICHTA, A. M. AND GOLDBERG, J. M. Afferent and efferent responses from morphological fiber classes in the turtle posterior crista. *Ann. NY Acad. Sci.* 781: 183–195, 1996.

BRICHTA, A. M. AND PETERSON, E. H. Functional architecture of vestibular primary afferents from the posterior semicircular canal of a turtle, *Pseudemys* (*Trachemys*) *scripta elegans. J. Comp. Neurol.* 344: 481–507, 1994.

CASTON, J. AND BRICOUT-BERTHOUT, A. Responses to somatosensory input by afferent and efferent neurons in the vestibular nerve of the frog. *Brain Behav. Evol.* 24: 135–143, 1984.

DAVIS, J. C. *Statistics and Data Analysis in Geology*. New York: Wiley-Interscience, 1973.

DECHESNE, C., RAYMOND, J., AND SANS, A. The efferent vestibular system in the cat: a horseradish peroxidase and fluorescent retrograde tracers study. *J. Neurosci*. 11: 893–901, 1984.

DEMEMES, D., WENTHOLD, R. J., MONIOT, B., AND SANS, A. Glutamate-like immunoreactivity in the peripheral vestibular system of mammals. *Hear. Res.* 46: 261–269, 1990.

DOI, K., TSUMOTO, T., AND MATSUNAGA, T. Actions of excitatory amino acid antagonists on synaptic inputs to the rat medial vestibular nucleus: an electrophysiological study in vitro. *Exp. Brain Res.* 82: 254–262, 1990.

FERNANDEZ, C., BAIRD, R. A., AND GOLDBERG, J. M. The vestibular nerve of the chinchilla. I. Peripheral innervation patterns in the horizontal and superior semicircular canals. *J. Neurophysiol.* 60: 167–181, 1988.

FERNANDEZ, C., LYSAKOWSKI, A., AND GOLDBERG, J. M. Hair-cell counts and afferent innervation patterns in the cristae ampullares of the squirrel monkey with a comparison to the chinchilla. *J. Neurophysiol.* 73: 1253–1269, 1995.

FRIEDMANN, I. AND BALLANTYNE, J. *Ultrastructural Atlas of the Inner Ear*. London: Butterworths, 1984, p. 211–244.

GACEK, R. R. Afferent and efferent innervation of the labyrinth. *Adv. Otorhinolaryngol.* 28: 1–13, 1982.

GACEK, R. R. AND LYON, M. The localization of vestibular efferent neurons in the kitten with horseradish peroxidase. *Acta Otolaryngol. (Stockh.)* 77: 92–101, 1974.

GLASER, J. R. AND GLASER, E. M. Neuron imaging with Neurolucida—a PC-based system for image combining microscopy. *Comput. Med. Imaging Graph.* 14: 307–317, 1990.

GOLDBERG, J. M. AND FERNANDEZ, C. Efferent vestibular system in the squirrel monkey: anatomical location and influence on afferent activity. *J. Neurophysiol.* 43: 986–1025, 1980.

GOLDBERG, J. M., LYSAKOWSKI, A., AND FERNANDEZ, C. Morphophysiological and ultrastructural studies in the mammalian cristae ampullares. *Hear. Res.* 49: 89–102, 1990.

GUINAN, J. J., JR. Physiology of olivocochlear efferents. In: *The Cochlea*, edited by P. Dallos, A. N. Popper, and R. R. Fay. Berlin: Springer-Verlag, 1996, p. 435–502.

GUINAN, J. J., JR., WARR, W. B., AND NORRIS, B. E. Differential olivocochlear projections from lateral versus medial zones of the superior olivary complex. *J. Comp. Neurol.* 221: 358–370, 1983.

GUINAN, J. J., JR., WARR, W. B., AND NORRIS, B. E. Topographic organization of the olivocochlear projections from the lateral and medial zones of the superior olivary complex. *J. Comp. Neurol.* 226: 21–27, 1984.

HIGHSTEIN, S. M. The central nervous system efferent control of the organs of balance and equilibrium. *Neurosci. Res.* 12: 13–30, 1991.

HIGHSTEIN, S. M. AND BAKER, R. Action of the efferent vestibular system

on primary afferents in the toadfish, *Opsanus tau*. *J. Neurophysiol.* 54: 370–384, 1985.

IGARASHI, M. AND YOSHINOBU, T. Comparative observations of the eminentia cruciata in birds and mammals (Abstract). *Anat. Rec.* 155: 269, 1966.

ISAAKS, E. H. AND MOHAN-SRIVASLAVA, R. *Applied Geostatistics*. London: Oxford Univ. Press, 1989.

ISHIYAMA, A., LOPEZ, I., AND WACKYM, P. A. Choline acetyltransferase immunoreactivity in the human vestibular end-organs. *Cell Biol. Int.* 18: 979–984, 1994.

KEVETTER, G. A. AND PERACHIO, A. A. Distribution of vestibular afferents that innervate the sacculus and posterior canal in the gerbil. *J. Comp. Neurol.* 254: 410–424, 1986.

LEWIS, E. R., LEVERENZ, E. L., AND BIALEK, W. B. *The Vertebrate Inner Ear*. Boca Raton, FL: CRC Press, 1985, p. 30–47.

LEWIS, M. R., PHELAN, K. D., SHINNICK-GALLAGHER, P., AND GALLAGHER, J. P. Primary afferent excitatory transmission recorded intracellularly in vitro from rat medial vestibular neurons. *Synapse* 3: 149–153, 1989.

LINDEMAN, H. H. Studies on the morphology of the sensory regions of the vestibular apparatus. *Ergeb. Anat. Entwicklungsgesch.* 42: 1–113, 1969.

LYSAKOWSKI, A., MINOR, L. B., FERNANDEZ, C., AND GOLDBERG, J. M. Physiological identification of morphologically distinct afferent classes innervating the cristae ampullares of the squirrel monkey. *J. Neurophysiol.* 73: 1270–1281, 1995.

MARCO, J., LEE, W. S., SUAREZ, C., HOFFMAN, L., AND HONRUBIA, V. Morphologic and quantitative study of the efferent vestibular system in the chinchilla—3-D reconstruction. *Acta Otolaryngol. (Stockh.)* 113: 229–234, 1993.

MCCUE, M. P. AND GUINAN, J. J. Influence of efferent stimulation on acoustically responsive vestibular afferents in the cat. *J. Neurosci.* 14: 6071–6083, 1994.

OHNO, K., TAKEDA, N., TANAKA-TSUJI, M., AND MATSUNAGA, T. Calcitonin gene-related peptide in the efferent system of the inner ear. *Acta Otolaryngol. Suppl. (Stockh.)* 501: 16–20, 1993.

PERACHIO, A. A. AND KEVETTER, G. A. Identification of vestibular efferent neurons in the gerbil: histochemical and retrograde labeling. *Exp. Brain Res.* 78: 315–326, 1989.

PURCELL, I. M. AND PERACHIO, A. A. Regional distributions of efferent neurons in the semicircular canals of the gerbil. *Ann. NY Acad. Sci.* 781: 680–682, 1996.

RAYMOND, J. AND DEMEMES, D. Efferent innervation of vestibular receptors in the cat: a radioautographic visualization. *Acta Otolaryngol. (Stockh.)* 96: 413–419, 1983.

ROBERTSON, D., COLE, K. S., AND CORBETT, K. Quantitative estimate of bilaterally projecting medial olivocochlear neurons in the guinea pig brain stem. *Hear. Res.* 27: 177–181, 1987a.

ROBERTSON, D., COLE, K. S., AND HARVEY, A. R. Brain stem organization of efferent projections to the guinea pig cochlea studied using the fluorescent tracers fast blue and diamidino yellow. *Exp. Brain Res.* 66: 449–457, 1987b.

ROSSI, M. L. AND MARTINI, M. Efferent control of posterior canal afferent receptor discharge in the frog labyrinth. *Brain Res.* 555: 123–134, 1991.

RYAN, A. F., SCHWARTZ, I. R., HELFERT, R. H., KEITHLEY, E. M., AND WANG, Z.-X. Selective retrograde labeling of lateral olivocochlear neurons in brain stem based on preferential uptake of ^{3}H-D-aspartic acid in the cochlea. *J. Comp. Neurol.* 255: 606–616, 1987.

RYAN, A. F., SCHWARTZ, I. R., KEITHLEY, E. M., AND WANG, Z.-X. Selective retrograde transport of nipecotic acid, a GABA analog, labels a subpopulation of gerbil olivocochlear neurons. *J. Comp. Neurol.* 326: 337–346, 1992.

RYAN, A. F., SIMMONS, D. M., WATTS, A. G., AND SWANSON, L. W. Enkephalin mRNA production by cochlear and vestibular efferent neurons in the gerbil brainstem. *Exp. Brain Res.* 87: 259–267, 1991.

SANS, A. AND HIGHSTEIN, S. H. New ultrastructural features in the vestibular labyrinth of the toadfish, *Opsanus tau*. *Brain Res.* 308: 191–195, 1984.

SCHNEIDER, L. W. AND ANDERSON, D. J. Transfer characteristics of first and second order lateral canal vestibular neurons in gerbil. *Brain Res.* 112: 61–76, 1976.

SCHWARTZ, I. R. AND RYAN, A. F. Amino acid labeling patterns in the innervation of the cochlea: an electron microscopic autoradiographic study. *J. Comp. Neurol.* 246: 500–512, 1986.

SCHWARZ, D.W.F., SATOH, K., SCHWARZ, I. E., AND HU, K. Vestibular and cochlear efferent neurons in the rat's brain stem. In: *The Vestibular System: Neurophysiologic and Clinical Research*, edited by M. D. Graham and J. L. Kemink. New York: Raven, 1987, p. 643–649.

SCHWARZ, I. E., SCHWARZ, D. W., FREDRICKSON, J. M., AND LANDOLT, J. P. Efferent vestibular neurons: a study employing retrograde tracer methods in the pigeon (*Columba livia*). *J. Comp. Neurol.* 196: 1–12, 1981.

SMITH, C. A. AND RASMUSSEN, G. Nerve endings in the maculae and cristae of the chinchilla vestibule, with special reference to the efferents. In: *Symposium on Role of Vestibular Organs in Exploration of Space*, Washington, DC: US Govt. Printing Office, 1968, p. 188–207.

TANAKA, M., TAKEDA, N., SENBA, E., TOHYAMA, M., KUBO, T., AND MATSUNAGA, T. Localization of calcitonin gene-related peptide in the vestibular end-organs in the rat: an immunohistochemical study. *Brain Res.* 447: 175–177, 1988.

TANAKA, M., TAKEDA, N., SENBA, E., TOHYAMA, M., KUBO, T., AND MATSUNAGA, T. Localization and origins of calcitonin gene-related peptide containing fibers in the vestibular end-organs of the rat. *Acta Otolaryngol. Suppl. (Stockh.)* 468: 31–34, 1989.

USAMI, S., IGARASHI, M., AND THOMPSON, G. C. GABA-like immunoreactivity in the squirrel monkey vestibular end organs. *Brain Res.* 417: 367–370, 1987.

VEENMAN, C. L., REINER, A., AND HONIG, M. G. Biotinylated dextran amine as an anterograde tracer for single- and double-labeling studies. *J. Neurosci. Methods* 413: 239–254, 1992.

VETTER, D. E., ADAMS, J. C., AND MUGNAINI, E. Chemically distinct rat olivocochlear neurons. *Synapse* 7: 21–43, 1991.

WACKYM, P. A. Ultrastructural organization of calcitonin gene-related peptide immunoreactive efferent axons and terminals in the vestibular periphery. *Am. J. Otol.* 14: 41–50, 1993.

WARR, W. B. Olivocochlear and vestibular efferent neurons of the feline brain stem: their location, morphology and number determined by retrograde axonal transport and acetylcholinesterase histochemistry. *J. Comp. Neurol.* 161: 159–172, 1975.

WARR, W. B. AND GUINAN, J. J., JR. Efferent innervation of the organ of Corti: two separate systems. *Brain Res.* 173: 152–155, 1979.

WHITE, J. S. Fine structure of vestibular efferent neurons in the albino rat. *Soc. Neurosci. Abstr.* 91.11: 322, 1985.

WHITE, J. S. AND WARR, W. B. The dual origins of the olivocochlear bundle in the albino rat. *J. Comp. Neurol.* 219: 203–214, 1983.